Acta Cryst E CRYSTALLOGRAPHIC COMMUNICATIONS

ISSN 2056-9890

Synthesis, crystal structure and Hirshfeld analysis of the bis{(*E*)-2-[1-(benzo[*d*][1,3]dioxol-5-yl)ethylidene]-*N*-ethylhydrazine-1-carbothioamide-κ*S*}dichloridomercury(II) complex

Renan Lira de Farias,[a] Johannes Beck,[b] Jörg Daniels[b] and Adriano Bof de Oliveira[c]*

[a]Departamento de Química, Pontifícia Universidade Católica do Rio de Janeiro, Rua Marquês de São Vicente 225, 22451-900 Rio de Janeiro-RJ, Brazil, [b]Institut für Anorganische Chemie, Rheinische Friedrich-Wilhelms-Universität Bonn, Gerhard-Domagk-Strasse 1, D-53121 Bonn, Germany, and [c]Núcleo de Química, Universidade Federal do Rio Grande, Avenida Itália km 08, 96203-900 Rio Grande-RS, Brazil. *Correspondence e-mail: adriano@furg.br

Received 16 April 2026
Accepted 8 May 2026

Edited by C. Schulzke, Universität Greifswald, Germany

Keywords: crystal structure; thiosemicarbazone complex; mercury(II) complex; H-bonded chelate-type; H-bonded intramolecular rings.

CCDC reference: 2552717

Supporting information: this article has supporting information at journals.iucr.org/e

The title compound, $[HgCl_2(C_{12}H_{15}N_3O_2S)_2]$, was synthesized by the reaction of (*E*)-2-[1-(benzo[*d*][1,3]dioxol-5-yl)ethylidene]-*N*-ethylhydrazine-1-carbothioamide [common name: 3′,4′-(methylenedioxy)acetophenone 4-ethylthiosemicarbazone] with mercury(II) chloride in a 2:1 molar ratio at ambient temperature, using ethanol as solvent. A white solid was isolated and colourless single crystals of the title compound for the SC-XRD analysis were obtained from a solution in (methanesulfinyl)methane (common name: dimethyl sulfoxide, DMSO) with a hexane overlay. The Hg^{II} metal center is fourfold coordinated in a distorted tetrahedral geometry by two neutral thiosemicarbazone derivatives, acting as κ*S*-donors, and two chlorido ligands. The complex molecule exhibits a sequence of four intramolecular hydrogen-bonded rings, formed by two interactions of the N—H···Cl type, with graph-set motifs of *S*(6) and showing a chelate-like coordination environment around the metal center, and two additional interactions of the N—H···N type with *S*(5) graph-set motifs. In the crystal, the molecules are linked *via* N—H···Cl intermolecular interactions along the *c*-axis, forming a hydrogen-bonded ribbon-like supramolecular arrangement that resembles a zigzag pattern along the *c*-axis direction, and with the Cl atoms acting as bridges between intra- and intermolecular hydrogen bonds. The Hirshfeld surface analysis suggests that the major contributions for the crystal cohesion are the H···H (40.4%), H···Cl/Cl···H (14.5%), H···C/C···H (11.3%), H···O/O···H (10.6%) and H···S/S···H (9.2%) intermolecular contacts, with the surface being mapped over the d_{norm}, shape-index and curvedness properties.

1. Chemical context

Thiosemicarbazone derivatives, from now on TSCs, are organic molecules with the functional group $R_1R_2C{=}N{-}(H)N{-}C(=S){-}NR_3R_4$ and were first reported by Freund & Schander (1902) as products of a synthetic methodology for the organic qualitative analysis of aldehydes and ketones. For example, the thiosemicarbazide molecule, $H_2N{-}N(H){-}C(=S){-}NH_2$, was employed as an analytical reagent for the detection of $R_1R_2C{=}O$ and $R_1HC{=}O$ functional groups, with the respective TSC and H_2O as products of the reaction. This classic condensation reaction with a nucleophilic attack from a Lewis base ($H_2N{-}R$) to a carbonyl group ($C{=}O$) remains up to the present time a standard synthetic methodology for new compounds with a wide range of applications in several disciplines, including medicinal chemistry.

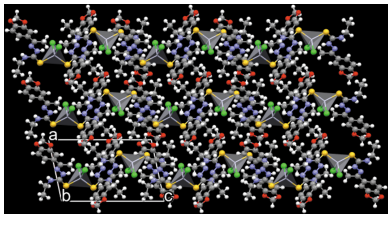

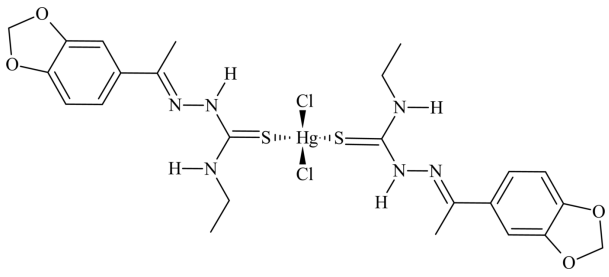

To the best of our knowledge, one of the first reports regarding the biological activity of TSCs, in this case for tuberculosis therapy, was published by Domagk *et al.* (1946). For other examples of the biological activities of TSCs and related compounds, see: Gupta *et al.* (2022); Khan *et al.* (2022); Pavan *et al.* (2010) and Parrilha *et al.* (2022).

Concerning the application of TSCs on coordination chemistry, some of the first reports are from Neuberg & Neimann (1902), describing the synthesis of TSC compounds with Ag^{I}, and Kuhn & Zilliken (1954), showing the synthesis of TSC ligands with Cu^{II} for medicinal applications. For a review addressing complexes with TSC ligands, see: Lobana *et al.* (2009).

As part of our work on the TSCs coordination chemistry, we report herein the synthesis, crystal structure and Hirshfeld analysis of the title compound, from now on **$HgCl_2(TSC1)_2$**, including a discussion about the intramolecular hydrogen bonds and their effects on the coordination sphere of TSC complexes with mercury(II) metal centers and chlorido ligands.

2. Structural commentary

The asymmetric unit of the title compound matches the molecular formula, with all atoms located in general positions. The Hg^{II} metal center is fourfold coordinated in a distorted tetrahedral geometry by two 3′,4′-(methylenedioxy)acetophenone 4-ethylthiosemicarbazones, **TSC1**, and two chlorido ligands (Fig. 1). The bond lengths and angles of the coordination sphere are in agreement with literature data for similar compounds and the respective values are given in Tables 1 and 2. For the Hg^{II} environment, a chelate-type coordination mode can be suggested based on the intramolecular hydrogen-bonds, N2—H2*N*···Cl2 and N5—H5*N*···Cl1, with graph-set motifs of *S*(6), resulting in two six-membered H-based metallarings. As a result of these structural features, the spatial orientation of the **TSC1** ligands in the title compound can be assumed as a *V*-shape (Fig. 2). The formation of intramolecular hydrogen bonds contributes to the thermodynamic stability of the molecules (Koll *et al.*, 2006; Steiner, 2002) and it can be suggested that they compensate possible steric hindrance effects and lower molecular symmetry, being a key structural feature for the complex addressed in this work. Additionally, two potential, albeit at rather acute angles, hydrogen-bonding contacts of the N—H···N type, *viz*,

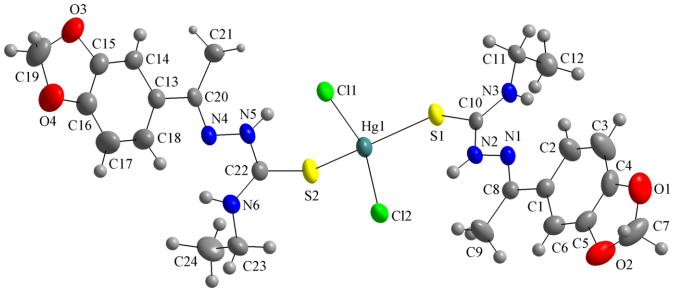

Figure 1
The molecular structure of the title compound showing the atom labelling for all non-hydrogen atoms. The displacement ellipsoids are drawn at the 35% probability level and the H atoms are drawn in the ball-and-stick model for clarity.

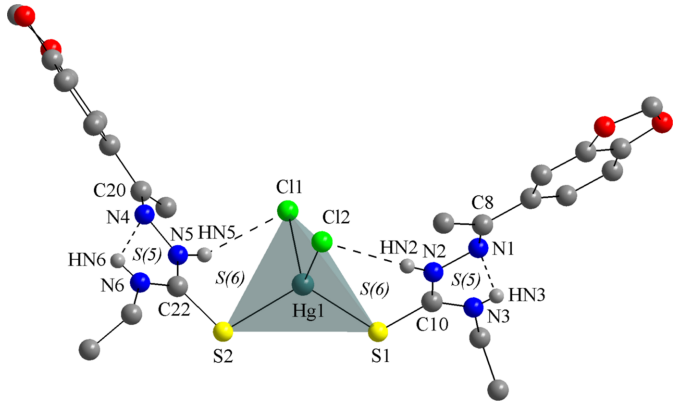

Figure 2
The molecular structure of the title compound presented as ball-and-stick model, with the H···Cl and H···N intramolecular interactions drawn as dashed lines and forming a sequence of four hydrogen-bonded rings with graph-set motifs of *S*(5) and *S*(6). The *S*(6) motifs resemble a hydrogen-based chelate-like coordination environment. The distorted tetrahedral coordination polyhedron is drawn with 70% transparency and only key atoms are labelled. The figure is simplified for clarity.

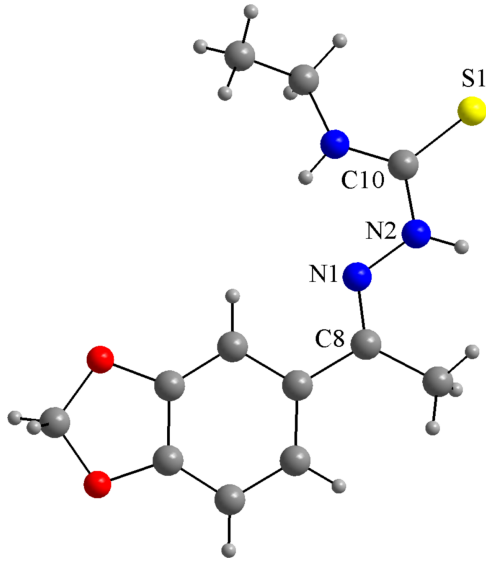

Figure 3
The molecular structure of **TSC1** (CUCZUX; de Oliveira *et al.*, 2015) drawn as a ball-and-stick model and with only key atoms labelled. The disorder of the ethyl moiety is omitted for clarity.

Table 1
Selected bond lengths (Å) of the title compound and from literature data.

Compounds	CSD refcodes	Chemical bonds	Bond lengths	Chemical bonds	Bond lengths
$HgCl_2(TSC1)_2$[a]	This work	N1—N2	1.390 (6)	N4—N5	1.399 (6)
		N2—C10	1.349 (7)	N5—C22	1.353 (7)
		C10—S1	1.725 (5)	C22—S2	1.720 (6)
		Hg1—Cl1	2.5681 (15)	Hg1—Cl2	2.5132 (15)
		Hg1—S1	2.4832 (14)	Hg1—S2	2.4878 (16)
TSC1[b]	CUCZUX	N1—N2	1.3730 (18)		
		N2—C10	1.358 (2)		
		C10—S1	1.6792 (17)		
$HgCl_2(TSC2)_2$[c]	EFUKEX	N3—N2	1.383 (4)	N13—N12	1.393 (4)
		N2—C1	1.330 (4)	N12—C11	1.307 (5)
		C1—S1	1.740 (3)	C11—S11	1.732 (4)
		Hg1—Cl1	2.7490 (8)	Hg1—Cl2	2.5947 (9)
		Hg1—S1	2.4049 (10)	Hg1—S11	2.4192 (9)
$HgCl_2(TSC3)_2$[d]	IRETOP	N2—N3	1.367 (10)	N5—N6	1.375 (9)
		N2—C11	1.342 (12)	N5—C27	1.321 (10)
		C11—S1	1.710 (9)	C27–S3	1.721 (9)
		Hg1—Cl1	2.397 (4)	Hg1—Cl2	2.607 (3)
		Hg1—S1	2.533 (3)	Hg1—S3	2.496 (2)
$HgCl_2(TSC4)_2$[e]	MOCXAH	N1—N2	1.392 (6)		
		N2—C16	1.328 (6)		
		C16—S1	1.715 (4)		
		Hg—Cl1	2.5177 (12)	Hg—S1	2.4975 (12)
$Hg_2Cl_4(TSC5)_2$[f]	GUTLEN	N1—N2	1.379 (4)		
		N2—C2	1.343 (4)		
		C2—S1	1.727 (3)		
		Hg1—Cl1	3.0387 (12)	Hg1—S1	2.3732 (8)
		Hg1—N1	2.748 (3)		
		Hg2—Cl1	2.4888 (12)	Hg2—Cl2	2.4653 (10)

Notes: (*a*) this work [TSC1 is 3′,4′-(methylenedioxy)acetophenone 4-ethylthiosemicarbazone]; (*b*) de Oliveira *et al.* (2015); (*c*) Trzesowska-Kruszynska (2014) (TSC2 is *p*-dimethylaminobenzaldehyde thiosemicarbazone); (*d*) Basu & Das (2011) [TSC3 is 2-thiophenealdehyde-*N*(4)-naphthylthiosemicarbazone]; (*e*) Nath & Baruah (2023) [TSC4 is 2-(anthracen-9-ylmethylene)-*N*-phenylthiosemicarbazone]; (*f*) López-Torres & Mendiola (2010) [TSC5 is benzaldehyde-*N*(4),*N*(4)-dimethylthiosemicarbazone].

Table 2
Selected bond angles (°) for the coordination sphere of Hg^{II} complexes with chlorido and thiosemicarbazone ligands.

Compounds	CSD refcodes	Chemical bonds	Angles
$HgCl_2(TSC1)_2$[a]	This work	S1—Hg1—S2	117.71 (5)
		Cl2—Hg1—S1	109.19 (5)
		Cl1—Hg1—S1	109.03 (5)
		Cl1—Hg1—S2	108.61 (5)
		Cl2—Hg1—S2	107.93 (6)
		Cl1—Hg1—Cl2	103.42 (6)
$HgCl_2(TSC2)_2$[b]	EFUKEX	S1—Hg1—S11	150.70 (4)
		Cl2—Hg1—S11	93.18 (4)
$HgCl_2(TSC3)_2$[c]	IRETOP	Cl1—Hg1—S3	119.21 (17)
		Cl1—Hg1—Cl2	99.30 (12)
$HgCl_2(TSC4)_2$[d]	MOCXAH	Cl^{i}—Hg—$S1^{i}$	114.71 (4)
		S1—-Hg—$S1^{i}$	105.43 (6)
$Hg_2Cl_4(TSC5)_2$[e]	GUTLEN	Cl1—Hg1—N1	109.65 (7)
		N1—Hg1—S1	106.72 (6)
		Cl1—Hg1—N1	79.48 (3)
		Cl1—Hg2—Cl2	110.65 (4)
		Hg1—Cl1—Hg2	90.29 (4)

Notes: (*a*) this work [TSC1 is 3′,4′-(methylenedioxy)acetophenone 4-ethylthiosemicarbazone]; (*b*) Trzesowska-Kruszynska (2014) (TSC2 is *p*-dimethylaminobenzaldehyde thiosemicarbazone); (*c*) Basu & Das (2011) [TSC3 is 2-thiophenealdehyde-*N*(4)-naphthylthiosemicarbazone]; (*d*) Nath & Baruah (2023) [TSC4 is 2-(anthracen-9-ylmethylene)-*N*-phenylthiosemicarbazone]; (*e*) López-Torres & Mendiola (2010) [TSC5 is benzaldehyde-*N*(4),*N*(4)-dimethylthiosemicarbazone]. Symmetry code: (i) $-x+\frac{3}{2}, y, -z+1$.

N3—H*N*3···N1 and N6—H*N*6···N4, with graph-set motifs *S*(5), are observed, forming a sequence of four hydrogen-bonded rings connected through the N2—C10 and N5—C22 bonds (Fig. 2 and Table 3).

One thiosemicarbazone fragment is almost planar, with the maximum deviation of the mean plane through the C8/N1/N2/C10/S1/N3 atoms being 0.0817 (39) Å for N1 (r.m.s.d. = 0.0449 Å). The entire ligand, however, is not planar due to the

Table 3
Hydrogen-bond geometry (Å, °).

D—H···*A*	*D*—H	H···*A*	*D*···*A*	*D*—H···*A*
C7—H7*B*···$S1^{i}$	0.97	2.85	3.642 (8)	139
C9—H9*C*···Cl2	0.96	2.89	3.474 (7)	121
C21—H21*A*···Cl1	0.96	2.90	3.675 (6)	139
C21—H21*B*···$Cl2^{ii}$	0.96	2.95	3.707 (6)	136
N2—H*N*2···Cl2	0.83 (5)	2.53 (5)	3.354 (5)	170 (4)
N3—H*N*3···$Cl1^{iii}$	0.76 (5)	2.68 (5)	3.293 (5)	140 (4)
N3—H*N*3···N1	0.76 (5)	2.22 (5)	2.604 (6)	113 (4)
N5—H*N*5···Cl1	0.85 (7)	2.53 (7)	3.233 (6)	141 (6)
N6—H*N*6···$Cl2^{iv}$	0.87 (6)	2.58 (6)	3.300 (5)	141 (5)
N6—H*N*6···N4	0.87 (6)	2.19 (6)	2.649 (7)	112 (5)
C23—H23*A*···S2	0.96 (6)	2.60 (6)	3.134 (8)	115 (4)
C24—H24*A*···$Cl2^{iv}$	1.21 (7)	2.77 (7)	3.739 (9)	137 (4)
C24—H24*B*···$O3^{v}$	1.01 (7)	2.60 (7)	3.513 (11)	151 (6)

Symmetry codes: (i) $-x+1, -y, -z$; (ii) $x, y+1, z$; (iii) $-x+1, -y+1, -z$; (iv) $-x+1, -y+1, -z-1$; (v) $-x+1, -y+2, -z-1$.

angle between the plane through the thiosemicarbazone moiety and the plane of the respective aromatic ring, which amounts to 16 (3)°, and the torsion angle regarding the terminal ethyl fragment, C10—N3—C11—C12, of −93.9 (8)°. The other thiosemicarbazone ligand is also not planar, with the C20/N4/N5/C22/S2 moiety showing the maximum deviation of the mean plane through the selected atoms of 0.1524 (39) Å for N4 (r.m.s.d. = 0.0774 Å), the angle between this plane and the respective aromatic ring of 31.4 (3)°, and the torsion angle regarding the respective ethyl group, C22—N6—C23—C24, being −106.9 (8)°.

The neutral form of **TSC1** is evident in the presence of the hydrazinic hydrogen atoms, H*N*2 and H*N*5, and the well-defined N—N, N—C and C═S bonds (Table 2; CSD refcode: CUCZUX; de Oliveira *et al.*, 2015; Fig. 3). In the deprotonated thiosemicarbazones, the hydrazinic H atom is removed and the resulting negative charge is delocalized over the N—C—S chain, in which the bond lengths tend to converge, with the N—N and N—C entities showing a double bond character and the C—S acquiring a single bond character (DAWTAZ; de Oliveira *et al.*, 2017 and TOKDUU; de Oliveira *et al.*, 2014). In the title compound, the C═S bond lengths are slightly longer than the respective bond in the crystal structure of the free ligand, **TSC1**, and this effect can be understood by the coordination of the thiocarbonyl groups to the metal center. The polarization of the electron density of the sulfur atoms toward the metal ion affects the C—S bond distances, as observed for similar compounds (Table 1). This effect is observed even for neutral TSC ligands, where the C—S bonds will not become single ones, but the related interatomic distances will increase by *ca*. 0.1 Å, which is a typical structural feature for these complexes.

3. Supramolecular features

In the crystal, the molecules of the title compound are connected *via* N—H···Cl intermolecular interactions, building a one-dimensional ribbon-like supramolecular arrangement along the *c*-axis direction in which the Cl atoms act as bridges for intra- and intermolecular hydrogen bonds, namely, H*N*3···Cl1^{i}···H*N*5^{i} and H*N*6···Cl2^{ii}···H*N*2^{ii} [symmetry codes: (i) $-x+1, -y+1, -z-1$; (ii) $-x+1, -y+1, -z$] and the interaction angles amount to 157.087 (3) and 170.750 (3)°, respectively (Fig. 4, Table 3). The H···Cl interatomic distances range from 2.55 to 2.79 Å, being shorter than the sum of the van der Waals radii for the respective atoms (2.95 Å according to Bondi, 1964; 2.86 Å by Rowland & Taylor, 1996; from 2.86 Å to 3.06 Å, as compiled by Batsanov, 2001). In addition, concerning the supramolecular arrangement of the title compound, a zigzag pattern along the *c*-axis direction is observed in a 3 × 3 × 3 expanded unit cell, when viewed along the *b* axis (Fig. 5).

An analysis of the intermolecular interactions of the title compound was further performed with a Hirshfeld surface (Hirshfeld, 1977) evaluation, including the two-dimensional Hirshfeld surface fingerprints (HSFP) of the major contributions for the crystal cohesion and the graphical representations of the surface mapped over the d_{norm}, shape-index and curvedness properties (Mackenzie *et al.*, 2017; Turner *et al.*, 2017). The most important contributions to the crystal packing are from H···H (40.4%), H···Cl/Cl···H (14.5%), H···C/C···H (11.3%), H···O/O···H (10.6%) and H···S/S···H (9.2%) intermolecular contacts. To complete the series with hydrogen atoms, the H···N/N···H (3.9%) contacts were included in the analysis and the results are presented in a single figure, with the contact types and contributions given within the graphics (Fig. 6). The Hirshfeld surface mapped over d_{norm} shows in red the regions related to strong intermolecular contacts, corresponding in this work to the regions around the H3*N*, H6*N*, Cl1 and Cl2 atoms, as shown in Fig. 7(*a*). The surface regions drawn in blue and white indicate

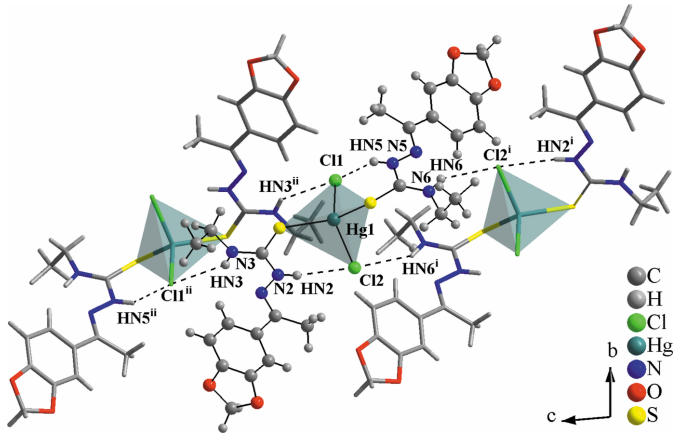

Figure 4
Section of the crystal structure of the title compound viewed along the *a* axis, showing the H···Cl interactions drawn as dashed lines and the molecules linked into an 1-D ribbon-like supramolecular arrangement along the *c*-axis direction. The asymmetric unit is presented as a ball-and-stick model, the distorted tetrahedral coordination polyhedra are drawn with 70% transparency, and the figure is simplified for clarity. [Symmetry codes: (i) $-x+1, -y+1, -z-1$; (ii) $-x+1, -y+1, -z$.]

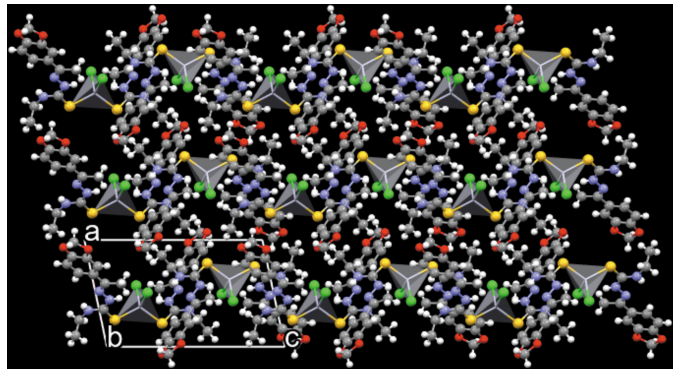

Figure 5
Graphical representation of the 3 × 3 × 3 expanded unit cell of the title compound viewed along the *b* axis, showing a zigzag pattern for the supramolecular arrangement along the *c*-axis direction. For clarity, the molecules are drawn using the ball-and-stick model and the coordination polyhedra are shown with 80% transparency.

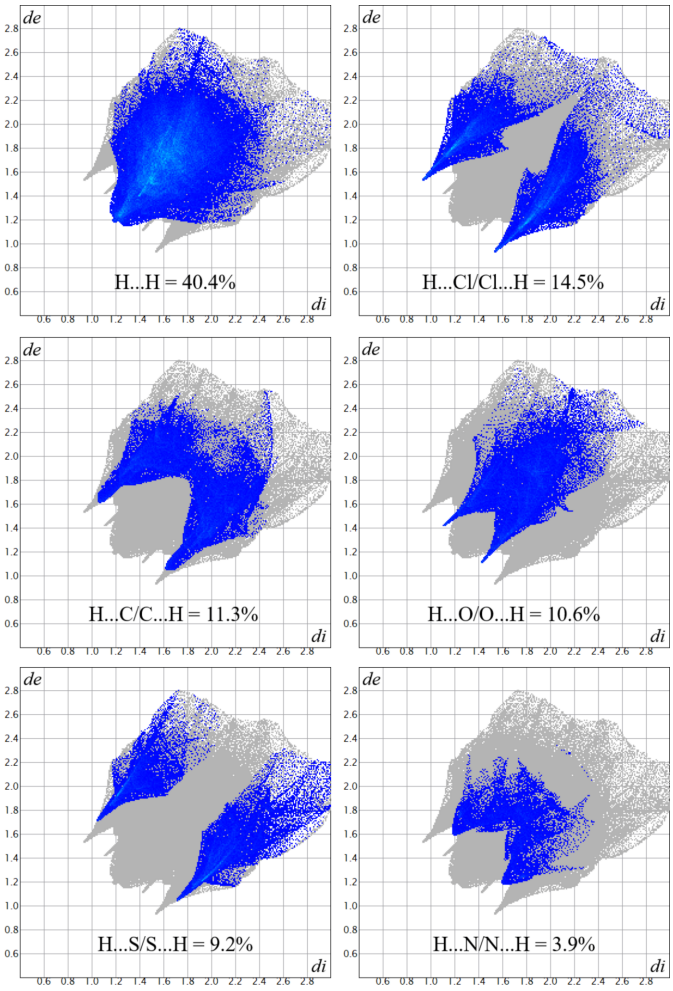

Figure 6
The HSFP-graphical representation of selected intermolecular interaction contributions for the crystal cohesion of the title compound. Interactions are highlighted in blue tones and contribution values (in %) are given within the figure. The d_e and d_i components are given in Å.

locations with weak or irrelevant intermolecular interactions. The surface mapping set to the shape-index mode indicates the regions of the donor atoms in blue and concave local surfaces and the regions of the acceptor ones in red and convex surfaces. In the crystal structure of the title compound, the regions around the H atoms are related to the donor atoms and the regions around the Cl atoms mainly as acceptors, as depicted in Fig. 7(*b*). Finally, the surface mapped over curvedness indicates regions proper for intermolecular interactions as flat local surfaces, while regions in which close contacts are precluded are shown as surfaces with irregularities or vertices. For example, the local surfaces over the aromatic rings are not flat, which suggests that intermolecular interactions such as π–π-stacking are strongly unlikely, as observed in Fig. 7(*c*).

4. Database survey

The database survey for the title compound was performed with the Cambridge Structural Database (CSD, accessed *via* the WebCSD tool on April 10, 2026; Groom *et al.*, 2016) and the *ConQuest* software (Version 2025.2.0, accessed on April 10, 2026; Bruno *et al.*, 2002), being refined with the following parameters: two neutral thiosemicarbazone fragments acting as κS-donors and two chlorido ligands coordinated to an Hg^{II} metal center. The survey returned only four crystal structures, *viz.* the complex with the *p*-dimethylaminobenzaldehyde thiosemicarbazone derivative, **$HgCl_2(TSC2)_2$**, (EFUKEX; Trzesowska-Kruszynska, 2014), the complex with 2-thiophenealdehyde-*N*(4)-naphthylthiosemicarbazone, **$HgCl_2(TSC3)_2$**, (IRETOP; Basu & Das, 2011), the complex with 2-(anthracen-9-ylmethylene)-*N*-phenylthiosemicarbazone, **$HgCl_2(TSC4)_2$**, (MOCXAH; Nath & Baruah, 2023) and the complex with benzaldehyde-*N*(4),*N*(4)-dimethylthiosemicarbazone, **$Hg_2Cl_4(TSC5)_2$**, (GUTLEN; López-Torres & Mendiola, 2010).

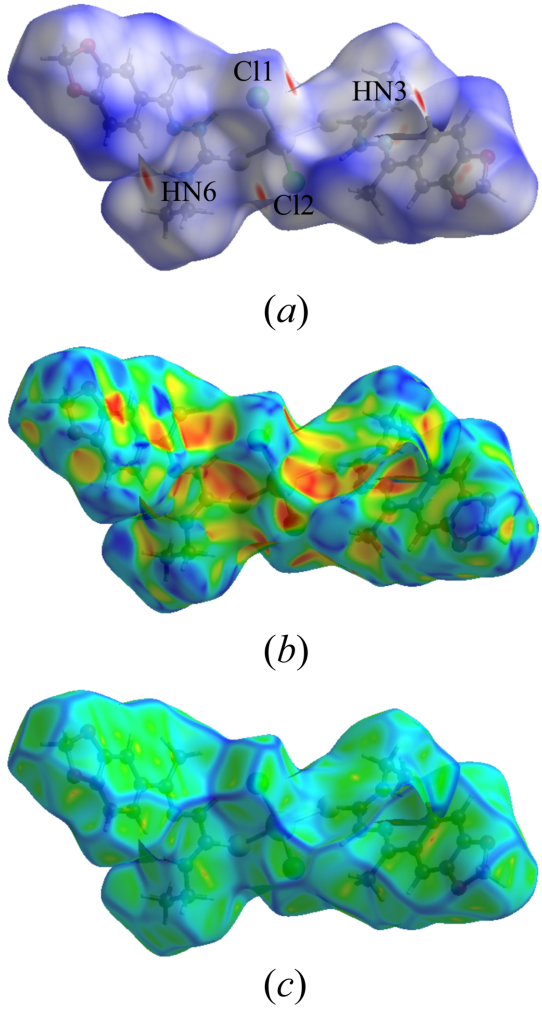

Figure 7
Graphical representations of the Hirshfeld surfaces of the title compound mapped over the following properties: (*a*) d_{norm} (range: 0,2655 to 1,4904 a.u.), with key atoms labelled and regions with strong intermolecular contacts drawn in red, (*b*) shape-index (range: −1.0000 to 1.0000 a.u.), with the blue/concave regions for the donor atoms, the red/convex ones for acceptor atoms, and (*c*) curvedness (range: −4.0000 to 0.4000 a. u.), showing vertices and irregularities over the aromatic rings, suggesting that short-range interactions such as π–π contacts are absent.

Table 4
Hydrogen-bond geometry (Å, °) for the reference Hg^{II} complexes with chlorido and thiosemicarbazone ligands.

Compounds	CSD refcodes	D—H···A	D—H	H···A	D···A	D—H···A
$HgCl_2(TSC2)_2$[a]	EFUKEX	N1—H1*N*···Cl1^{i}	0.88	2.6242 (8)	3.4124 (3)	149.68 (20)
		N1—H1*O*···Cl2^{i}	0.88	2.3794 (10)	3.2212 (32)	160.17 (20)
		N1—H1*N*···N3	0.88	2.2978 (29)	2.6384 (42)	102.98 (21)
		N11—H11*O*···Cl2^{ii}	0.88	2.3555 (10)	3.2033 (38)	161.46 (23)
		N11—H11*N*···N13	0.88	2.2785 (30)	2.6241 (47)	103.26 (23)
		N12—H12*N*···Cl1	0.88	2.4057 (8)	3.2590 (29)	163.72 (18)
		N2—H2*N*···Cl1	0.88	2.3960 (8)	3.1684 (32)	146.66 (20)
$HgCl_2(TSC3)_2$[b]	IRETOP	N1—H1N···N3	0,88	2.1704 (83)	2.5671 (13)	107.82 (55)
		N2—H2*N*···Cl2	0.86	2.3558 (28)	3.2123 (96)	172.06 (62)
		N4—H4*N*···N6	0.88	2.2738 (83)	2.6350 (13)	105.31 (51)
		N5—H5*N*···Cl2	0.86	2.4030 (22)	3.2541 (66)	169.71 (41)
$HgCl_2(TSC4)_2$[c]	MOCXAH	N2—H2···Cl1	0.86	2.4803 (13)	3.2444 (47)	148.37 (30)
		N3—H3···Cl1^{iii}	0.86	2.6802 (12)	3.3786 (32)	139.25 (20)
		N3—H3···N1	0.86	2.3039 (35)	2.6597 (46)	105.04 (22)

Notes: (*a*) Trzesowska-Kruszynska (2014) (TSC2 is *p*-dimethylaminobenzaldehyde thiosemicarbazone); (*b*) Basu & Das (2011) [TSC3 is 2-thiophenealdehyde-*N*(4)-naphthylthiosemicarbazone]; (*c*) Nath & Baruah (2023) [TSC4 is 2-(anthracen-9-ylmethylene)-*N*-phenylthiosemicarbazone]. Symmetry codes: (i) $x+1, y, z$; (ii) $x, -y+\frac{3}{2}, z+\frac{1}{2}$; (iii) $x-\frac{1}{2}, -y+1, z$.

For the molecular structures of **$HgCl_2(TSC2)_2$** (Fig. 8), **$HgCl_2(TSC3)_2$** (Fig. 9) and **$HgCl_2(TSC4)_2$** (Fig. 10), the Hg^{II} metal center is fourfold coordinated by two neutral thiosemicarbazones acting as κS-donors and two chlorido ligands, exhibiting a similar coordination environment as observed for the title compound (Figs. 1 and 2). The distorted tetrahedral geometries are assured by the respective Hg—Cl and Hg—S bond lengths (Table 1) and the selected bond angles (Table 2).

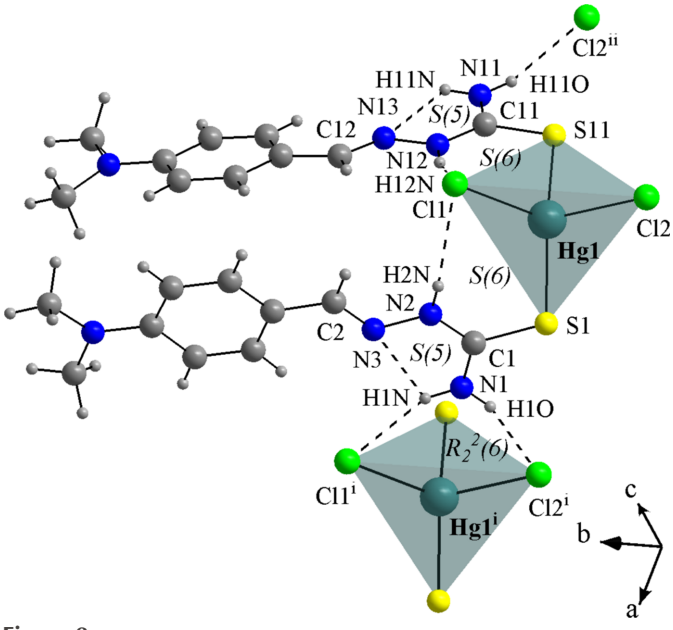

Figure 8
Section of the crystal structure of **$HgCl_2(TSC2)_2$** (EFUKEX; Trzesowska-Kruszynska, 2014), with the H-bonding being drawn as dashed lines. The structure is expanded by the N1—H1*N*···Cl^{i} and N1—H1*O*···Cl2^{i} interactions, forming a graph-set motif of $R_2^2(6)$ and a chelate-type environment for the Hg1^{i} center, and by the N11—H11*O*···Cl2^{ii} interaction into a hydrogen-bonded tape-like supramolecular arrangement along the *ac*-plane. A ball-and-stick model is used for the graphical representation, which is simplified for clarity. Only key atoms are labelled and the distorted tetrahedral coordination polyhedra are drawn with 70% transparency. [Symmetry codes: (i) $x+1, y, z$; (ii) $x, -y+\frac{3}{2}, z+\frac{1}{2}$.]

For the title compound, all bond angles in the coordination sphere are reported, while for the **$HgCl_2(TSC2)_2$**, **$HgCl_2(TSC3)_2$** and **$HgCl_2(TSC4)_2$** complexes, only the maximal and the minimal values are given. The molecular structure of **$Hg_2Cl_4(TSC5)_2$** has a totally different coordination environment for the metal centers, being a dinuclear complex (Fig. 11), and the data given in Tables 1 and 2 refer to the asymmetric unit only.

The hydrogen-bonding geometries observed for the **$HgCl_2(TSC2)_2$**, **$HgCl_2(TSC3)_2$** and **$HgCl_2(TSC4)_2$** complexes (Figs. 8, 9 and 10; Table 4) adopt a pattern very similar to the title compound. This molecular arrangement includes two intramolecular interactions of the N—H···Cl type, with $S(6)$ graph-set motifs forming a chelate-like coordination environment around the metal center. Two additional interactions of the N—H···N type, with $S(5)$ graph-set motif may be considered. It must be pointed out, though, that for the three

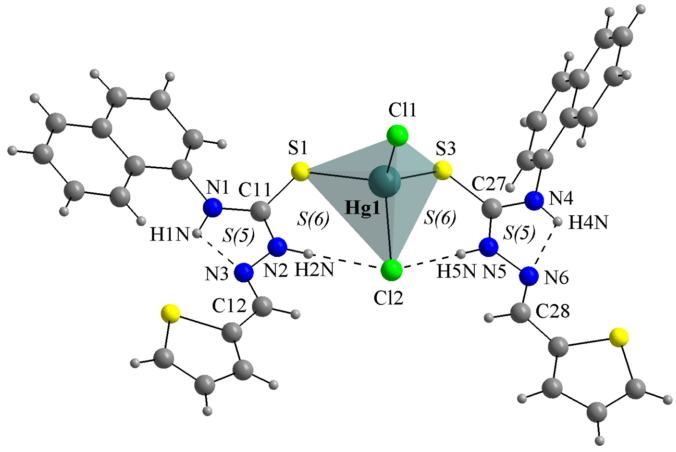

Figure 9
The molecular structure of **$HgCl_2(TSC3)_2$** (IRETOP; Basu & Das, 2011). The intramolecular hydrogen bonds are drawn as dashed lines. A ball-and-stick model is used for the graphical representation; only key atoms are labelled and the distorted tetrahedral coordination polyhedron is drawn with 70% transparency for clarity.

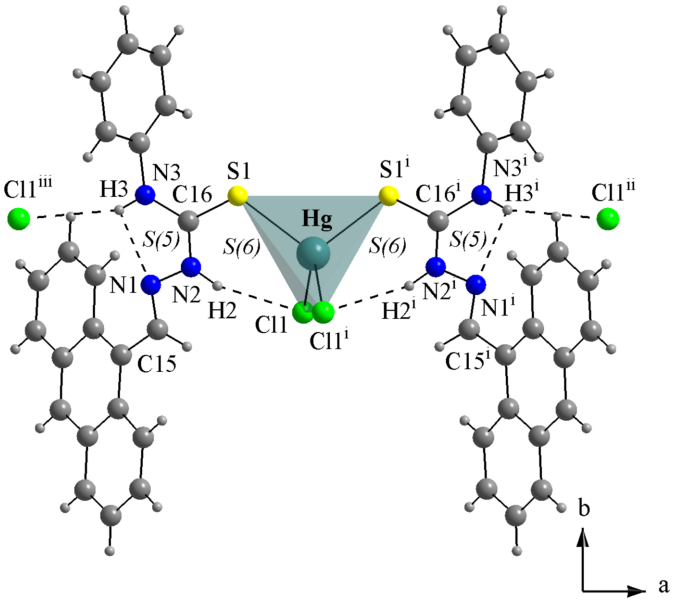

Figure 10
Crystal structure section of **$HgCl_2$(TSC4)$_2$** (MOCXAH; Nath & Baruah, 2023), in which the H-bonding is drawn as dashed lines. The molecules are linked by N—H···Cl interactions, building a 1-D ribbon-like supramolecular arrangement along the *a*-axis direction. A ball-and-stick model is used for the graphical representation; only key atoms are labelled and the distorted tetrahedral coordination polyhedron is drawn with 70% transparency for clarity. [Symmetry codes: (i) $-x+\frac{3}{2}, y, -z+1$; (ii) $-x+2, -y+1, -z+1$; (iii) $x-\frac{1}{2}, -y+1, z$.]

molecules from the database the respective angles are even more acute than in the title compound, ranging from 103 to 108°. For **$HgCl_2$(TSC2)$_2$** and **$HgCl_2$(TSC3)$_2$**, the TSCs are oriented to the same side of the respective molecules, possibly

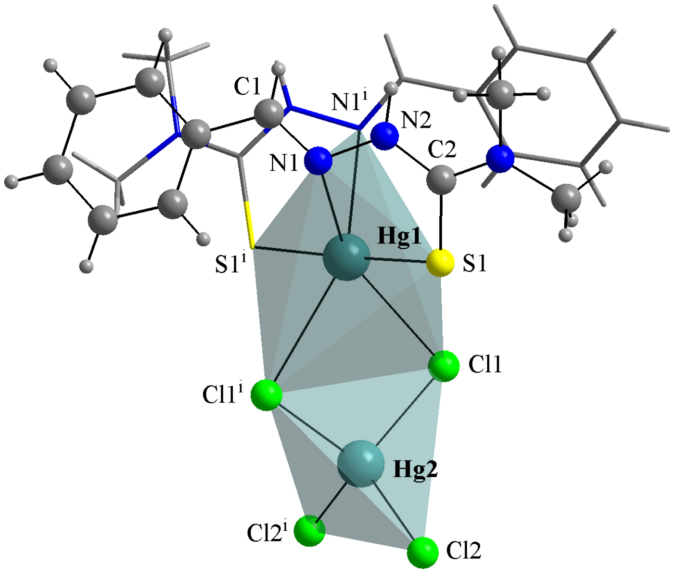

Figure 11
The molecular structure of **Hg_2Cl_4(TSC5)$_2$** (GUTLEN; López-Torres & Mendiola, 2010). A ball-and-stick model is used for the graphical representation; only key atoms are labelled and the distorted coordination polyhedra are drawn with 70% transparency for clarity. [Symmetry code: (i) $-x, y, -z+\frac{1}{2}$.]

due to the H2*N*···Cl1···H12*N* and H2*N*···Cl2···H5*N* intramolecular bridges. Regarding the supramolecular arrangements, the **$HgCl_2$(TSC2)$_2$** molecules are linked by N—H···Cl intermolecular interactions into a tape-like structure along the *ac*-plane (Fig. 8, Table 4), while the **$HgCl_2$(TSC4)$_2$** molecules are connected by the same type of intermolecular interactions observed in this work, forming a one-dimensional ribbon-like structure along the *a*-axis direction (Fig. 10, Table 4). Neither strong nor relevant intermolecular interactions were observed for **$HgCl_2$(TSC3)$_2$** and therefore only weak intermolecular interactions, *e.g.*, the London dispersion forces can be suggested. Thus, the molecules can be presented as discrete units in the crystal structure (for a graphical representation, see the supporting information). N.B. the *D*—H bond lengths in Table 4 were obtained directly from deposited data (984145, 793913 and 2233994 CIF files from CCDC *via* www.ccdc.cam.ac.uk/structures) while the other values were measured using *DIAMOND 3.2* (Brandenburg, 2006).

Lastly, in **Hg_2Cl_4(TSC5)$_2$** one Hg^{II} metal center is coordinated by two neutral thiosemicarbazone derivatives in a chelate mode, acting as *κN*,*S*-donors, and by two chlorido ligands, forming a six-vertex polyhedron resembling a strongly distorted octahedron. The second Hg^{II} center is coordinated by four chlorido ligands in a distorted tetrahedral geometry (Fig. 11). The mercury(II) centers are connected by Cl atoms acting as bridges, *viz.* Hg1—Cl1—Hg2 and Hg1—Cl1^{i}—Hg2, with the bond angle being 90.29 (4)° [symmetry code: (i) $-x, y, -z+\frac{1}{2}$]. Selected bond lengths and angles for comparison with the title compound and a neutral thiosemicarbazone derivative are given in Tables 1 and 2. Even though the molecular structure of **Hg_2Cl_4(TSC5)$_2$** does not exhibit intramolecular hydrogen bonding and cannot contribute to the discussion about their effects on the coordination and molecular geometries of TSC complexes addressed in this work, the report from López-Torres & Mendiola (2010) is still a notable reference for $Hg_xCl_y(TSC)_2$ compounds.

5. Synthesis and crystallization

The starting materials are commercially available and were used without further purification. The **TSC1** ligand was obtained as previously reported (de Oliveira *et al.*, 2015) and suspended in ethanol (1 mmol, 0.2653 g in 50 mL) under magnetic stirring at room temperature. Under the same conditions, a suspension of mercury(II) chloride in ethanol was prepared (0.5 mmol, 0.1357 g in 50 mL). The solutions were combined and stirred at room temperature for 4 h, after which a white solid was formed, and afterwards isolated by filtration. The one-step synthesis was adapted from literature procedures (Basu & Das, 2011; López-Torres & Mendiola, 2010; Nath & Baruah, 2023). The solid was washed with small portions of cold ethanol and dried at room temperature. As a result of the non-uniformity of the bulk white solid, the purification of the product and the yield determination were not possible. Colourless single crystals suitable for X-ray diffraction were obtained in a test tube from a solution of the

Table 5
Experimental details.

Crystal data	
Chemical formula	$[HgCl_2(C_{12}H_{15}N_3O_2S)_2]$
M_r	802.15
Crystal system, space group	Triclinic, $P\overline{1}$
Temperature (K)	293
a, b, c (Å)	9.4412 (5), 10.4130 (5), 15.4626 (8)
α, β, γ (°)	94.616 (3), 101.797 (3), 91.079 (3)
V (Å^3)	1482.24 (13)
Z	2
Radiation type	Mo $K\alpha$
μ (mm^{-1})	5.55
Crystal size (mm)	0.08 × 0.08 × 0.07
Data collection	
Diffractometer	Enraf–Nonius FR590 Kappa CCD
Absorption correction	Analytical [using the algorithm from de Meulenaer & Tompa (1965), in Alcock (1970)]
T_{min}, T_{max}	0.634, 0.724
No. of measured, independent and observed [$I > 2\sigma(I)$] reflections	17004, 5627, 3849
R_{int}	0.064
(sin $\theta/\lambda)_{max}$ (Å^{-1})	0.611
Refinement	
$R[F^2 > 2\sigma(F^2)]$, $wR(F^2)$, S	0.036, 0.074, 0.97
No. of reflections	5627
No. of parameters	434
H-atom treatment	H atoms treated by a mixture of independent and constrained refinement
$\Delta\rho_{max}$, $\Delta\rho_{min}$ (e Å^{-3})	0.53, −1.29

Computer programs: *COLLECT* (Nonius, 1998), *HKL*, *DENZO* and *SCALEPACK* (Otwinowski & Minor, 1997), *SIR92* (Altomare *et al.*, 1994), *SHELXL2019/3* (Sheldrick, 2015), *CrystalExplorer 17.5* (Mackenzie *et al.*, 2017; Turner *et al.* 2017), *DIAMOND* (Brandenburg, 2006), *Mercury* (Macrae *et al.*, 2020), *WinGX* (Farrugia, 2012), *enCIFer* (Allen *et al.*, 2004) and *publCIF* (Westrip, 2010).

solid in dimethyl sulfoxide with a hexane overlay after some weeks.

6. Refinement

Crystal data, data collection and structure refinement details are summarized in Table 5. The structure solution was performed using direct methods and refined on F^2 with anisotropic displacement factors for the non-hydrogen atoms. The H-atoms were treated by a mixture of constrained and independent refinement. The H atoms attached to C7, C9, C19 and C21 (Fig. 1) were positioned with idealized geometry and refined applying the HFIX instruction, with U_{iso}(H) = 1.2 U_{eq} (C7/C19 atoms) and U_{iso}(H) = 1.5 U_{eq} (C9/C21 atoms), with bond lengths set to C—H = 0.97 and 0.96 Å, respectively. The remaining hydrogen atoms were located in difference-Fourier maps and freely refined with isotropic displacement parameters. The C—H bond lengths in the aromatic rings range from 0.87 (6) Å for C6—H6 to 1.05 (6) Å for C17—H17, while the values for the ethyl entities range from 0.90 (7) Å for C23—H23*B* to 1.21 (7) Å for C24—H24*A*. The N—H bond lengths range from 0.76 (5) Å, N3—H*N*3, to 0.87 (6) Å, N6—H*N*6. Planes through selected atoms, torsion angles and the hydrogen-bond geometries were calculated with the MPLA, CONF and HTAB instructions. Only classical hydrogen bonds were considered for the discussion in this work, while the complete dataset from the refinement is provided in Table 3.

Acknowledgements

We gratefully acknowledge financial support by the German Research Council (DFG) within the Collaborative Research Area SFB 813 – Chemistry at Spin Centers and by the State of North Rhine-Westphalia, Germany. ABO is a former DAAD scholarship holder and alumnus of the University of Bonn, Germany, and thanks both of these institutions for their long-time support.

Funding information

Funding for this research was provided by: Coordenação de Aperfeiçoamento de Pessoal de Nível Superior – Brasil - (CAPES) – Finance Code 001 ; Fundação Carlos Chagas Filho de Amparo à Pesquisa do Estado do Rio de Janeiro - Brasil - (FAPERJ) (grant No. E-26/211.027/2024 to R. L. de Farias).

References

Alcock, N. W. (1970). *Crystallographic Computing* edited by F. R. Ahmed, S. R. Hall & C. P. Huber, pp. 271–278. Copenhagen, Denmark: Munksgaard.
Allen, F. H., Johnson, O., Shields, G. P., Smith, B. R. & Towler, M. (2004). *J. Appl. Cryst.* **37**, 335–338.
Altomare, A., Cascarano, G., Giacovazzo, C., Guagliardi, A., Burla, M. C., Polidori, G. & Camalli, M. (1994). *J. Appl. Cryst.* **27**, 435–436.
Basu, A. & Das, G. (2011). *Inorg. Chim. Acta* **372**, 394–399.
Batsanov, S. S. (2001). *Inorg. Mater.* **37**, 871–885.
Bondi, A. (1964). *J. Phys. Chem.* **68**, 441–451.
Brandenburg, K. (2006). *DIAMOND*. Crystal Impact GbR, Bonn, Germany.
Bruno, I. J., Cole, J. C., Edgington, P. R., Kessler, M., Macrae, C. F., McCabe, P., Pearson, J. & Taylor, R. (2002). *Acta Cryst.* B**58**, 389–397.
Domagk, G., Behnisch, R., Mietzsch, F. & Schmidt, H. (1946). *Naturwissenschaften* **33**, 315.
Farrugia, L. J. (2012). *J. Appl. Cryst.* **45**, 849–854.
Freund, M. & Schander, A. (1902). *Ber. Dtsch. Chem. Ges.* **35**, 2602–2606.
Groom, C. R., Bruno, I. J., Lightfoot, M. P. & Ward, S. C. (2016). *Acta Cryst.* B**72**, 171–179.
Gupta, S., Singh, N., Khan, T. & Joshi, S. (2022). *Results Chem.* **4**, 100459.
Hirshfeld, H. L. (1977). *Theor. Chim. Acta* **44**, 129–138.
Khan, T., Raza, S. & Lawrence, A. J. (2022). *Russ. J. Coord. Chem.* **48**, 877–895.
Koll, A., Karpfen, A. & Wolschann, P. (2006). *J. Mol. Struct.* **790**, 55–64.
Kuhn, R. & Zilliken, F. (1954). United States Patent and Trademark Office Patent No. US-2695911-A/2,695,911.
Lobana, T. S., Sharma, R., Bawa, G. & Khanna, S. (2009). *Coord. Chem. Rev.* **253**, 977–1055.
López-Torres, E. & Mendiola, M. A. (2010). *Inorg. Chim. Acta* **363**, 1275–1283.
Mackenzie, C. F., Spackman, P. R., Jayatilaka, D. & Spackman, M. A. (2017). *IUCrJ* **4**, 575–587.
Macrae, C. F., Sovago, I., Cottrell, S. J., Galek, P. T. A., McCabe, P., Pidcock, E., Platings, M., Shields, G. P., Stevens, J. S., Towler, M. & Wood, P. A. (2020). *J. Appl. Cryst.* **53**, 226–235.

Meulenaer, J. de & Tompa, H. (1965). *Acta Cryst.* **19**, 1014–1018.
Nath, J. & Baruah, J. B. (2023). *ACS Omega* **8**, 42827–42839.
Neuberg, C. & Neimann, W. (1902). *Ber. Dtsch. Chem. Ges.* **35**, 2049–2056.
Nonius (1998). *COLLECT*. Nonius BV, Delft, The Netherlands.
Oliveira, A. B. de, Beck, J., Mellone, S. E. B. S. & Daniels, J. (2017). *Acta Cryst.* E**73**, 859–863.
Oliveira, A. B. de, Feitosa, B. R. S., Näther, C. & Jess, I. (2014). *Acta Cryst.* E**70**, 101–103.
Oliveira, A. B. de, Lira de Farias, R., Näther, C. & Jess, I. (2015). *Acta Cryst.* E**71**, o208–o209.
Otwinowski, Z. & Minor, W. (1997). *Methods in Enzymology* Vol. 276, *Macromolecular Crystallography* Part A, edited by C. W. Carter Jr & R. M. Sweet, pp. 307–326. New York: Academic Press.
Parrilha, G. L., dos Santos, R. G. & Beraldo, H. (2022). *Coord. Chem. Rev.* **458**, 214418.
Pavan, F. R., Maia, P. I. S., Leite, S. R. A., Deflon, V. M., Batista, A. A., Sato, D. N., Franzblau, S. G. & Leite, C. Q. F. (2010). *Eur. J. Med. Chem.* **45**, 1898–1905.
Rowland, R. S. & Taylor, R. (1996). *J. Phys. Chem.* **100**, 7384–7391.
Sheldrick, G. M. (2015). *Acta Cryst.* C**71**, 3–8.
Steiner, T. (2002). *Angew. Chem. Int. Ed.* **41**, 48–76.
Trzesowska-Kruszynska, A. (2014). *J. Mol. Struct.* **1072**, 284–290.
Turner, M. J., McKinnon, J. J., Wolff, S. K., Grimwood, D. J., Spackman, P. R., Jayatilaka, D. & Spackman, M. A. (2017). *CrystalExplorer17*. University of Western Australia, Perth, Australia.
Westrip, S. P. (2010). *J. Appl. Cryst.* **43**, 920–925.

supporting information

Acta Cryst. (2026). E**82**, 656-664 [https://doi.org/10.1107/S2056989026004822]

Synthesis, crystal structure and Hirshfeld analysis of the bis{(*E*)-2-[1-(benzo[*d*][1,3]dioxol-5-yl)ethylidene]-*N*-ethylhydrazine-1-carbothioamide-*κS*}dichloridomercury(II) complex

Renan Lira de Farias, Johannes Beck, Jörg Daniels and Adriano Bof de Oliveira

Computing details

Bis{(*E*)-2-[1-(benzo[*d*][1,3]dioxol-5-yl)ethylidene]-*N*-ethylhydrazine-1-carbothioamide-*κS*}dichloridomercury(II)

Crystal data

$[HgCl_2(C_{12}H_{15}N_3O_2S)_2]$
M_r = 802.15
Triclinic, $P\overline{1}$
a = 9.4412 (5) Å
b = 10.4130 (5) Å
c = 15.4626 (8) Å
α = 94.616 (3)°
β = 101.797 (3)°
γ = 91.079 (3)°
V = 1482.24 (13) Å^3
Z = 2
$F(000)$ = 788
D_x = 1.797 Mg m^{-3}
Mo $K\alpha$ radiation, λ = 0.71073 Å
Cell parameters from 37747 reflections
θ = 2.9–25.7°
μ = 5.55 mm^{-1}
T = 293 K
Block, colourless
0.08 × 0.08 × 0.07 mm

Data collection

Enraf–Nonius FR590 Kappa CCD diffractometer
Radiation source: sealed X-ray tube, Enraf–Nonius FR590
Horizontally mounted graphite crystal monochromator
Detector resolution: 9 pixels mm^{-1}
CCD rotation images, thick slices, κ–goniostat scans
Absorption correction: analytical [using the algorithm from de Meulenaer & Tompa (1965), in Alcock (1970)]
T_{min} = 0.634, T_{max} = 0.724
17004 measured reflections
5627 independent reflections
3849 reflections with $I > 2\sigma(I)$
R_{int} = 0.064
θ_{max} = 25.7°, θ_{min} = 3.0°
h = −9→11
k = −12→12
l = −18→18

Refinement

Refinement on F^2
Least-squares matrix: full
$R[F^2 > 2\sigma(F^2)]$ = 0.036
$wR(F^2)$ = 0.074
S = 0.97
5627 reflections
434 parameters
0 restraints
Primary atom site location: structure-invariant direct methods
Secondary atom site location: difference Fourier map
Hydrogen site location: mixed
H atoms treated by a mixture of independent and constrained refinement

$w = 1/[\sigma^2(F_o^2) + (0.0254P)^2]$
where $P = (F_o^2 + 2F_c^2)/3$
$(\Delta/\sigma)_{max} < 0.001$

$\Delta\rho_{max} = 0.53$ e Å^{-3}
$\Delta\rho_{min} = -1.29$ e Å^{-3}

Special details

Geometry. All esds (except the esd in the dihedral angle between two l.s. planes) are estimated using the full covariance matrix. The cell esds are taken into account individually in the estimation of esds in distances, angles and torsion angles; correlations between esds in cell parameters are only used when they are defined by crystal symmetry. An approximate (isotropic) treatment of cell esds is used for estimating esds involving l.s. planes.

Fractional atomic coordinates and isotropic or equivalent isotropic displacement parameters (Å^2)

	x	*y*	*z*	U_{iso}*/U_{eq}
C1	0.3201 (6)	0.0745 (5)	−0.0107 (4)	0.0493 (15)
C2	0.3079 (9)	0.1267 (7)	0.0731 (5)	0.075 (2)
C3	0.2253 (10)	0.0656 (9)	0.1249 (6)	0.095 (3)
C4	0.1552 (7)	−0.0474 (7)	0.0891 (5)	0.069 (2)
C5	0.1682 (6)	−0.0989 (5)	0.0070 (5)	0.0578 (17)
C6	0.2461 (7)	−0.0429 (6)	−0.0440 (5)	0.0574 (18)
C7	0.0225 (9)	−0.2283 (7)	0.0626 (7)	0.102 (3)
H7A	−0.082097	−0.229416	0.043760	0.122*
H7B	0.049474	−0.308882	0.087752	0.122*
C8	0.4078 (6)	0.1421 (5)	−0.0636 (4)	0.0460 (14)
C9	0.4074 (9)	0.0888 (7)	−0.1563 (4)	0.086 (2)
H9A	0.325785	0.119674	−0.195928	0.130*
H9B	0.401075	−0.003678	−0.159620	0.130*
H9C	0.495177	0.116033	−0.172778	0.130*
C10	0.6490 (5)	0.4092 (5)	−0.0252 (3)	0.0381 (13)
C11	0.7496 (7)	0.5229 (6)	0.1225 (4)	0.0493 (15)
C12	0.8945 (8)	0.4736 (8)	0.1636 (6)	0.0673 (19)
C13	0.2798 (6)	0.9187 (5)	−0.5172 (4)	0.0486 (15)
C14	0.2181 (7)	1.0385 (6)	−0.5100 (4)	0.0508 (16)
C15	0.1042 (7)	1.0655 (6)	−0.5742 (4)	0.0562 (16)
C16	0.0471 (7)	0.9789 (7)	−0.6435 (5)	0.0688 (19)
C17	0.1021 (9)	0.8602 (8)	−0.6533 (5)	0.087 (3)
C18	0.2212 (8)	0.8313 (7)	−0.5881 (5)	0.071 (2)
C19	−0.0681 (8)	1.1626 (7)	−0.6631 (6)	0.094 (3)
H19A	−0.035336	1.217659	−0.703384	0.112*
H19B	−0.164525	1.187025	−0.657277	0.112*
C20	0.4050 (6)	0.8819 (5)	−0.4499 (3)	0.0451 (14)
C21	0.4509 (7)	0.9660 (5)	−0.3654 (4)	0.0616 (18)
H21A	0.415495	0.928486	−0.318813	0.092*
H21B	0.412063	1.049886	−0.372845	0.092*
H21C	0.554710	0.973733	−0.350127	0.092*
C22	0.6615 (6)	0.6425 (5)	−0.4229 (4)	0.0444 (14)
C23	0.7439 (9)	0.5099 (7)	−0.5426 (5)	0.0636 (19)
C24	0.8561 (9)	0.5668 (10)	−0.5836 (6)	0.086 (2)
HN2	0.547 (5)	0.304 (4)	−0.126 (3)	0.026 (14)*
HN3	0.620 (5)	0.374 (4)	0.080 (3)	0.025 (15)*

HN5	0.571 (7)	0.752 (6)	−0.348 (5)	0.08 (2)*
HN6	0.599 (7)	0.655 (6)	−0.542 (4)	0.07 (2)*
H2	0.367 (7)	0.206 (6)	0.097 (4)	0.08 (2)*
H3	0.223 (7)	0.104 (6)	0.182 (5)	0.08 (2)*
H6	0.243 (7)	−0.078 (6)	−0.097 (4)	0.07 (2)*
H11A	0.694 (5)	0.549 (4)	0.167 (3)	0.028 (13)*
H11B	0.757 (6)	0.600 (6)	0.094 (4)	0.064 (19)*
H12A	0.946 (6)	0.449 (5)	0.121 (4)	0.051 (18)*
H12B	0.968 (8)	0.563 (7)	0.197 (5)	0.12 (3)*
H12C	0.886 (7)	0.400 (6)	0.201 (4)	0.08 (2)*
H14	0.252 (7)	1.096 (6)	−0.469 (4)	0.07 (2)*
H17	0.043 (7)	0.792 (6)	−0.702 (4)	0.08 (2)*
H18	0.260 (6)	0.752 (6)	−0.589 (4)	0.060 (19)*
H23A	0.774 (6)	0.460 (6)	−0.493 (4)	0.065 (19)*
H23B	0.683 (7)	0.460 (6)	−0.584 (5)	0.09 (2)*
H24A	0.792 (7)	0.631 (6)	−0.640 (5)	0.09 (2)*
H24B	0.924 (8)	0.624 (6)	−0.537 (5)	0.09 (2)*
H24C	0.931 (9)	0.500 (8)	−0.616 (6)	0.13 (3)*
Cl1	0.42642 (16)	0.68707 (14)	−0.23721 (9)	0.0516 (4)
Cl2	0.4929 (2)	0.31509 (14)	−0.29256 (10)	0.0685 (5)
Hg1	0.62812 (3)	0.52412 (2)	−0.23243 (2)	0.05213 (10)
N1	0.4794 (5)	0.2433 (4)	−0.0241 (3)	0.0445 (11)
N2	0.5602 (5)	0.3131 (4)	−0.0711 (3)	0.0429 (12)
N3	0.6593 (5)	0.4255 (5)	0.0609 (3)	0.0427 (12)
N4	0.4667 (5)	0.7771 (5)	−0.4701 (3)	0.0472 (12)
N5	0.5754 (5)	0.7378 (5)	−0.4026 (3)	0.0503 (13)
N6	0.6554 (6)	0.6068 (5)	−0.5071 (3)	0.0524 (13)
O1	0.0695 (6)	−0.1239 (6)	0.1266 (4)	0.0980 (17)
O2	0.0884 (6)	−0.2141 (4)	−0.0112 (4)	0.0935 (17)
O3	0.0275 (5)	1.1772 (4)	−0.5793 (3)	0.0834 (15)
O4	−0.0707 (6)	1.0307 (5)	−0.6972 (4)	0.0996 (18)
S1	0.75042 (16)	0.50784 (14)	−0.07567 (9)	0.0506 (4)
S2	0.78087 (16)	0.58069 (17)	−0.33820 (10)	0.0586 (4)

Atomic displacement parameters (Å²)

	U^{11}	U^{22}	U^{33}	U^{12}	U^{13}	U^{23}
C1	0.049 (4)	0.044 (3)	0.054 (4)	−0.002 (3)	0.011 (3)	0.008 (3)
C2	0.092 (6)	0.077 (5)	0.055 (5)	−0.032 (4)	0.015 (4)	0.001 (4)
C3	0.107 (7)	0.117 (7)	0.062 (5)	−0.051 (6)	0.026 (5)	0.001 (5)
C4	0.065 (5)	0.074 (5)	0.074 (5)	−0.007 (4)	0.015 (4)	0.036 (4)
C5	0.047 (4)	0.042 (3)	0.088 (5)	−0.004 (3)	0.019 (4)	0.014 (3)
C6	0.054 (4)	0.052 (4)	0.067 (5)	−0.002 (3)	0.017 (4)	0.001 (4)
C7	0.078 (6)	0.058 (5)	0.185 (10)	0.007 (4)	0.053 (6)	0.032 (6)
C8	0.050 (4)	0.044 (3)	0.043 (3)	0.005 (3)	0.006 (3)	0.006 (3)
C9	0.128 (7)	0.079 (5)	0.050 (4)	−0.043 (5)	0.022 (4)	−0.007 (4)
C10	0.036 (3)	0.042 (3)	0.036 (3)	0.006 (2)	0.004 (2)	0.012 (2)
C11	0.055 (4)	0.056 (4)	0.036 (3)	−0.002 (3)	0.009 (3)	0.001 (3)

C12	0.055 (5)	0.082 (5)	0.065 (5)	0.003 (4)	0.012 (4)	0.010 (4)
C13	0.051 (4)	0.051 (4)	0.045 (4)	−0.003 (3)	0.010 (3)	0.009 (3)
C14	0.055 (4)	0.044 (4)	0.055 (4)	−0.004 (3)	0.013 (3)	0.008 (3)
C15	0.051 (4)	0.055 (4)	0.065 (4)	0.005 (3)	0.012 (3)	0.015 (3)
C16	0.064 (5)	0.073 (5)	0.064 (5)	0.007 (4)	0.000 (4)	0.010 (4)
C17	0.092 (6)	0.079 (5)	0.073 (5)	0.007 (5)	−0.019 (5)	−0.006 (4)
C18	0.079 (5)	0.063 (5)	0.063 (5)	0.015 (4)	−0.005 (4)	0.002 (4)
C19	0.070 (5)	0.074 (5)	0.131 (8)	0.009 (4)	−0.003 (5)	0.031 (5)
C20	0.057 (4)	0.047 (3)	0.034 (3)	−0.008 (3)	0.013 (3)	0.010 (3)
C21	0.079 (5)	0.051 (4)	0.050 (4)	0.004 (3)	0.003 (3)	0.000 (3)
C22	0.042 (3)	0.050 (3)	0.044 (4)	−0.001 (3)	0.013 (3)	0.011 (3)
C23	0.075 (5)	0.069 (5)	0.046 (4)	0.010 (4)	0.013 (4)	−0.002 (4)
C24	0.067 (5)	0.118 (7)	0.083 (6)	0.016 (5)	0.037 (5)	−0.003 (6)
Cl1	0.0573 (9)	0.0581 (9)	0.0434 (8)	0.0080 (7)	0.0164 (7)	0.0111 (7)
Cl2	0.1078 (14)	0.0508 (9)	0.0429 (9)	−0.0072 (9)	0.0067 (9)	0.0045 (7)
Hg1	0.06164 (17)	0.05620 (15)	0.04099 (14)	0.00356 (10)	0.01264 (10)	0.01320 (10)
N1	0.049 (3)	0.046 (3)	0.038 (3)	−0.001 (2)	0.006 (2)	0.011 (2)
N2	0.048 (3)	0.048 (3)	0.031 (3)	−0.001 (2)	0.005 (2)	0.005 (2)
N3	0.043 (3)	0.050 (3)	0.036 (3)	−0.010 (2)	0.007 (2)	0.010 (2)
N4	0.052 (3)	0.055 (3)	0.036 (3)	0.009 (2)	0.009 (2)	0.011 (2)
N5	0.056 (3)	0.063 (3)	0.032 (3)	0.005 (3)	0.008 (3)	0.011 (3)
N6	0.061 (3)	0.057 (3)	0.041 (3)	0.011 (3)	0.013 (3)	0.006 (3)
O1	0.094 (4)	0.109 (4)	0.100 (4)	−0.033 (3)	0.031 (3)	0.038 (3)
O2	0.088 (4)	0.057 (3)	0.146 (5)	−0.017 (3)	0.051 (4)	0.007 (3)
O3	0.077 (3)	0.070 (3)	0.099 (4)	0.023 (3)	0.000 (3)	0.022 (3)
O4	0.079 (4)	0.099 (4)	0.106 (4)	0.021 (3)	−0.021 (3)	0.017 (3)
S1	0.0488 (9)	0.0633 (9)	0.0398 (8)	−0.0082 (7)	0.0055 (7)	0.0165 (7)
S2	0.0478 (9)	0.0863 (12)	0.0470 (9)	0.0118 (8)	0.0132 (7)	0.0258 (8)

Geometric parameters (Å, º)

C1—C2	1.392 (9)	C15—C16	1.357 (9)
C1—C6	1.403 (8)	C15—O3	1.381 (7)
C1—C8	1.483 (8)	C16—C17	1.359 (10)
C2—C3	1.406 (10)	C16—O4	1.391 (8)
C2—H2	0.99 (6)	C17—C18	1.404 (9)
C3—C4	1.358 (10)	C17—H17	1.05 (6)
C3—H3	0.95 (7)	C18—H18	0.91 (6)
C4—O1	1.366 (8)	C19—O3	1.415 (8)
C4—C5	1.368 (9)	C19—O4	1.429 (8)
C5—C6	1.340 (9)	C19—H19A	0.9700
C5—O2	1.383 (7)	C19—H19B	0.9700
C6—H6	0.87 (6)	C20—N4	1.293 (7)
C7—O1	1.410 (10)	C20—C21	1.495 (7)
C7—O2	1.424 (10)	C21—H21A	0.9600
C7—H7A	0.9700	C21—H21B	0.9600
C7—H7B	0.9700	C21—H21C	0.9600
C8—N1	1.281 (6)	C22—N6	1.315 (7)

C8—C9	1.493 (8)	C22—N5	1.353 (7)
C9—H9A	0.9600	C22—S2	1.720 (6)
C9—H9B	0.9600	C23—N6	1.466 (8)
C9—H9C	0.9600	C23—C24	1.478 (11)
C10—N3	1.312 (7)	C23—H23A	0.96 (6)
C10—N2	1.349 (7)	C23—H23B	0.90 (7)
C10—S1	1.725 (5)	C24—H24A	1.21 (7)
C11—N3	1.464 (7)	C24—H24B	1.01 (7)
C11—C12	1.504 (9)	C24—H24C	1.16 (9)
C11—H11A	0.97 (5)	Cl1—Hg1	2.5681 (15)
C11—H11B	0.95 (6)	Cl2—Hg1	2.5133 (15)
C12—H12A	0.92 (6)	Hg1—S1	2.4832 (14)
C12—H12B	1.16 (8)	Hg1—S2	2.4878 (16)
C12—H12C	1.01 (7)	N1—N2	1.390 (6)
C13—C18	1.381 (8)	N2—HN2	0.83 (5)
C13—C14	1.393 (8)	N3—HN3	0.76 (5)
C13—C20	1.485 (8)	N4—N5	1.399 (6)
C14—C15	1.357 (8)	N5—HN5	0.85 (7)
C14—H14	0.84 (6)	N6—HN6	0.87 (6)

C2—C1—C6	118.3 (6)	C16—C17—H17	118 (3)
C2—C1—C8	120.8 (5)	C18—C17—H17	124 (3)
C6—C1—C8	121.0 (6)	C13—C18—C17	121.9 (7)
C1—C2—C3	122.3 (7)	C13—C18—H18	117 (4)
C1—C2—H2	116 (4)	C17—C18—H18	121 (4)
C3—C2—H2	121 (4)	O3—C19—O4	108.4 (5)
C4—C3—C2	116.9 (8)	O3—C19—H19A	110.0
C4—C3—H3	124 (4)	O4—C19—H19A	110.0
C2—C3—H3	119 (4)	O3—C19—H19B	110.0
C3—C4—O1	127.4 (8)	O4—C19—H19B	110.0
C3—C4—C5	120.7 (7)	H19A—C19—H19B	108.4
O1—C4—C5	111.9 (6)	N4—C20—C13	116.1 (5)
C6—C5—C4	123.8 (6)	N4—C20—C21	124.8 (5)
C6—C5—O2	128.3 (7)	C13—C20—C21	119.1 (5)
C4—C5—O2	107.9 (6)	C20—C21—H21A	109.5
C5—C6—C1	118.0 (7)	C20—C21—H21B	109.5
C5—C6—H6	118 (4)	H21A—C21—H21B	109.5
C1—C6—H6	123 (4)	C20—C21—H21C	109.5
O1—C7—O2	108.6 (6)	H21A—C21—H21C	109.5
O1—C7—H7A	110.0	H21B—C21—H21C	109.5
O2—C7—H7A	110.0	N6—C22—N5	118.0 (5)
O1—C7—H7B	110.0	N6—C22—S2	123.2 (5)
O2—C7—H7B	110.0	N5—C22—S2	118.7 (4)
H7A—C7—H7B	108.4	N6—C23—C24	113.1 (6)
N1—C8—C1	115.6 (5)	N6—C23—H23A	102 (4)
N1—C8—C9	125.4 (5)	C24—C23—H23A	118 (4)
C1—C8—C9	119.0 (5)	N6—C23—H23B	106 (5)
C8—C9—H9A	109.5	C24—C23—H23B	109 (5)

C8—C9—H9B	109.5	H23A—C23—H23B	107 (6)
H9A—C9—H9B	109.5	C23—C24—H24A	106 (3)
C8—C9—H9C	109.5	C23—C24—H24B	109 (4)
H9A—C9—H9C	109.5	H24A—C24—H24B	110 (5)
H9B—C9—H9C	109.5	C23—C24—H24C	120 (4)
N3—C10—N2	118.1 (5)	H24A—C24—H24C	108 (5)
N3—C10—S1	119.7 (4)	H24B—C24—H24C	105 (6)
N2—C10—S1	122.3 (4)	S1—Hg1—S2	117.71 (5)
N3—C11—C12	112.5 (6)	S1—Hg1—Cl2	109.19 (5)
N3—C11—H11A	106 (3)	S2—Hg1—Cl2	107.93 (6)
C12—C11—H11A	112 (3)	S1—Hg1—Cl1	109.03 (5)
N3—C11—H11B	110 (3)	S2—Hg1—Cl1	108.61 (5)
C12—C11—H11B	113 (4)	Cl2—Hg1—Cl1	103.42 (6)
H11A—C11—H11B	102 (4)	C8—N1—N2	118.3 (5)
C11—C12—H12A	111 (4)	C10—N2—N1	117.2 (5)
C11—C12—H12B	107 (4)	C10—N2—HN2	120 (3)
H12A—C12—H12B	97 (5)	N1—N2—HN2	122 (3)
C11—C12—H12C	112 (4)	C10—N3—C11	126.7 (5)
H12A—C12—H12C	109 (5)	C10—N3—HN3	115 (4)
H12B—C12—H12C	118 (5)	C11—N3—HN3	118 (4)
C18—C13—C14	119.0 (6)	C20—N4—N5	115.1 (5)
C18—C13—C20	119.3 (6)	C22—N5—N4	118.5 (5)
C14—C13—C20	121.7 (5)	C22—N5—HN5	117 (5)
C15—C14—C13	118.3 (6)	N4—N5—HN5	121 (5)
C15—C14—H14	119 (4)	C22—N6—C23	126.3 (6)
C13—C14—H14	123 (4)	C22—N6—HN6	112 (4)
C16—C15—C14	122.2 (6)	C23—N6—HN6	121 (4)
C16—C15—O3	110.2 (6)	C4—O1—C7	105.2 (6)
C14—C15—O3	127.5 (6)	C5—O2—C7	106.4 (6)
C15—C16—C17	121.9 (6)	C15—O3—C19	105.1 (5)
C15—C16—O4	109.8 (6)	C16—O4—C19	104.5 (5)
C17—C16—O4	128.3 (6)	C10—S1—Hg1	110.21 (18)
C16—C17—C18	116.7 (7)	C22—S2—Hg1	104.2 (2)

C6—C1—C2—C3	0.4 (11)	C14—C13—C20—C21	10.0 (8)
C8—C1—C2—C3	179.7 (7)	C1—C8—N1—N2	−178.1 (4)
C1—C2—C3—C4	−0.9 (13)	C9—C8—N1—N2	2.4 (9)
C2—C3—C4—O1	179.8 (7)	N3—C10—N2—N1	3.7 (7)
C2—C3—C4—C5	1.3 (13)	S1—C10—N2—N1	−177.4 (4)
C3—C4—C5—C6	−1.3 (12)	C8—N1—N2—C10	−171.7 (5)
O1—C4—C5—C6	179.9 (6)	N2—C10—N3—C11	179.6 (5)
C3—C4—C5—O2	178.7 (7)	S1—C10—N3—C11	0.7 (8)
O1—C4—C5—O2	0.0 (8)	C12—C11—N3—C10	−93.9 (8)
C4—C5—C6—C1	0.8 (10)	C13—C20—N4—N5	−174.3 (5)
O2—C5—C6—C1	−179.2 (6)	C21—C20—N4—N5	5.8 (8)
C2—C1—C6—C5	−0.4 (9)	N6—C22—N5—N4	11.4 (8)
C8—C1—C6—C5	−179.7 (6)	S2—C22—N5—N4	−172.4 (4)
C2—C1—C8—N1	5.8 (9)	C20—N4—N5—C22	−168.8 (5)

C6—C1—C8—N1	−174.9 (5)	N5—C22—N6—C23	177.1 (6)
C2—C1—C8—C9	−174.6 (6)	S2—C22—N6—C23	1.1 (9)
C6—C1—C8—C9	4.7 (9)	C24—C23—N6—C22	−106.9 (8)
C18—C13—C14—C15	−1.3 (9)	C3—C4—O1—C7	179.6 (8)
C20—C13—C14—C15	179.8 (6)	C5—C4—O1—C7	−1.7 (8)
C13—C14—C15—C16	1.5 (10)	O2—C7—O1—C4	2.8 (8)
C13—C14—C15—O3	179.6 (6)	C6—C5—O2—C7	−178.1 (7)
C14—C15—C16—C17	−0.8 (12)	C4—C5—O2—C7	1.8 (8)
O3—C15—C16—C17	−179.2 (7)	O1—C7—O2—C5	−2.9 (8)
C14—C15—C16—O4	178.1 (6)	C16—C15—O3—C19	−8.3 (8)
O3—C15—C16—O4	−0.3 (8)	C14—C15—O3—C19	173.4 (7)
C15—C16—C17—C18	0.0 (13)	O4—C19—O3—C15	13.6 (8)
O4—C16—C17—C18	−178.8 (7)	C15—C16—O4—C19	8.6 (8)
C14—C13—C18—C17	0.5 (11)	C17—C16—O4—C19	−172.5 (9)
C20—C13—C18—C17	179.5 (7)	O3—C19—O4—C16	−13.7 (8)
C16—C17—C18—C13	0.2 (13)	N3—C10—S1—Hg1	−153.3 (4)
C18—C13—C20—N4	11.1 (8)	N2—C10—S1—Hg1	27.9 (5)
C14—C13—C20—N4	−170.0 (5)	N6—C22—S2—Hg1	−132.1 (5)
C18—C13—C20—C21	−168.9 (6)	N5—C22—S2—Hg1	52.0 (5)

Hydrogen-bond geometry (Å, º)

D—H···*A*	*D*—H	H···*A*	*D*···*A*	*D*—H···*A*
C7—H7*B*···S1^{i}	0.97	2.85	3.642 (8)	139
C9—H9*C*···Cl2	0.96	2.89	3.474 (7)	121
C21—H21*A*···Cl1	0.96	2.90	3.675 (6)	139
C21—H21*B*···Cl2^{ii}	0.96	2.95	3.707 (6)	136
N2—H*N*2···Cl2	0.83 (5)	2.53 (5)	3.354 (5)	170 (4)
N3—H*N*3···Cl1^{iii}	0.76 (5)	2.68 (5)	3.293 (5)	140 (4)
N3—H*N*3···N1	0.76 (5)	2.22 (5)	2.604 (6)	113 (4)
N5—H*N*5···Cl1	0.85 (7)	2.53 (7)	3.233 (6)	141 (6)
N6—H*N*6···Cl2^{iv}	0.87 (6)	2.58 (6)	3.300 (5)	141 (5)
N6—H*N*6···N4	0.87 (6)	2.19 (6)	2.649 (7)	112 (5)
C23—H23*A*···S2	0.96 (6)	2.60 (6)	3.134 (8)	115 (4)
C24—H24*A*···Cl2^{iv}	1.21 (7)	2.77 (7)	3.739 (9)	137 (4)
C24—H24*B*···O3^{v}	1.01 (7)	2.60 (7)	3.513 (11)	151 (6)

Symmetry codes: (i) −*x*+1, −*y*, −*z*; (ii) *x*, *y*+1, *z*; (iii) −*x*+1, −*y*+1, −*z*; (iv) −*x*+1, −*y*+1, −*z*−1; (v) −*x*+1, −*y*+2, −*z*−1.